Penerbit Akademia Baru

Journal of Advanced Research in Fluid Mechanics and Thermal Sciences

Journal homepage: www.akademiabaru.com/arfmts.html
ISSN: 2289-7879

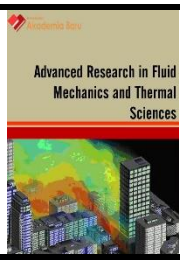

Flow and Wall Heat Transfer due to a Continuously Moving Slender Needle in Hybrid Nanofluid with Stability Analysis

Open Access

Siti Nur Alwani Salleh[1], Norfifah Bachok[1,2,*], Fadzilah Md Ali[1,2], Norihan Md Arifin[1,2]

[1] Institute for Mathematical Research, Universiti Putra Malaysia, 43400, UPM Serdang, Selangor, Malaysia
[2] Department of Mathematics, Faculty of Science, Universiti Putra Malaysia, 43400, UPM Serdang, Selangor, Malaysia

ARTICLE INFO

Article history:
Received 8 May 2020
Received in revised form 16 September 2020
Accepted 22 September 2020
Available online 25 October 2020

Keywords:
Hybrid nanofluid; dual solutions; stability analysis; numerical study

ABSTRACT

Present work deals with the numerical study of flow due to a continuously moving slender needle in a hybrid nanoliquid. The mathematical model of this work is developed in terms of nonlinear partial differential equations. By adopting the relevant similarity transformations, these equations are reduced to a system of nonlinear ordinary differential equations. Afterward, the solution is determined computationally via a bvp4c solver in MATLAB software. The influences of nanoparticle volume fraction, needle thickness and velocity ratio parameter on the rate of heat transfer, coefficient of skin friction, velocity as well as temperature distributions are illustrated in graphical form to describe the important features of the solution. The multiple solutions seem to appear when the needle opposes the free stream flow. It is revealed from the study that the composite (hybrid) nanoparticles augment the heat transfer rate between the flow and the needle in a certain domain of the velocity ratio parameter. The analysis of stability has proved that the upper branch solution represents stable flow, whereas the lower branch solution represents unstable flow.

1. Introduction

Along with the evolution of technologies, the well-known fluid, called hybrid nanofluid is being a potential fluid in order to enhance the performance of heat transfer. Hybrid nanoliquid is categorized as a new nanotechnology fluid where it is prepared by combining two types of nanoparticles into the conventional heat transfer fluids include ethylene glycol, kerosene, oil and water. Typically, one of these nanoparticles is non-metallic (such as Al_2O_3, CuO, MgO, and Fe_3O_4) and the other one is metallic (such as Ag, Al, Cu and Zn) in nature. In general, non-metallic nanoparticles provide lower thermal conductivity, yet they have a lot of beneficial properties like chemical inertness and stability. Contrarily, metallic nanoparticles have high thermal conductivities compared to non-metallic, but they have restrictions like reactivity and stability. Thus, the composition of these two types of

* *Corresponding author.*
E-mail address: norfifah@upm.edu.my

https://doi.org/10.37934/arfmts.76.3.6274

nanoparticles capable to increase the thermophysical properties and give an excellent thermal performance of the mixture. This behavior makes the hybrid nanoliquid is better than that of conventional coolant and nanoliquid with single nanoparticles.

Recently, it has been proved by the researchers that hybrid nanofluid can efficaciously replace the conventional heat transfer fluids, particularly for the technology that works at a very high temperature. Examples of the applications are manufacturing, biomedical, naval structures, transportation, acoustics, micro fluidics, electronic cooling, lubrication, solar heating, defence and space aircraft and ships. In recent years, many experimental studies [1-6] and numerical studies on the hybrid nanofluid have been considered by some authors. Takabi and Salehi [7] performed an analysis of the heat transfer of a hybrid nanoliquid on the sinusoidal corrugated enclosure. The influences of nanoliquid and hybrid nanoliquid are numerically studied by Moghadassi *et al.,* [8]. They concluded that the fluid that contains hybrid nanoparticles provides larger heat transfer coefficients. Devi and Devi [9] examined the performance of heat transfer for copper-alumina hybrid nanofluid past a stretched surface. Mehryan *et al.,* [10] considered the analysis of free convection embedded in a porous medium filled by hybrid nanoliquid. More researches on the hybrid nanoliquid problem are listed in the existing literature [11-16].

Nowadays, the consideration of the fluid flow induced by a slender needle seems to be an interesting topic in fluid dynamics. The investigation of the boundary layer flow due to a slender needle was initially introduced by Lee [17] in 1972. In the study, an approximation solution has been derived and the asymptotic features of the flow are discussed. According to Lee [17], the slender or thin needle has a parabolic revolution at its axes direction where its thicknesses are smaller or close to that of the boundary layer. This problem is quite interesting because of the motion of the slender needle that perturbs the direction of free stream flow. Such a situation is highly significant in experimental studies in order to compute the temperature and momentum profiles. Later on, the study of an isothermal thin needle in forced convection flow has been investigated by Narain and Uberoi [18]. Later on, Narain and Uberoi [19] performed the flow of mixed convection towards a slender needle by considering both isoflux and isothermal wall cases. Next, the steady viscous flow of non-isothermal slender needle is studied by Chen and Smith [20] considering the power-law surface temperature. The related problems involving the thin needle in a viscous fluid are reported in the published works of several authors [21-24].

The above-mentioned studies, however, restricted to the problem in a viscous fluid. Due to the existence of nanoparticles in the base fluid that enhances the heat transfer rate, hence, several studies have been done considering this fluid over a slender needle. The first problem of a slender needle in nanofluid was analyzed by Grosan and Pop [25]. In their studies, they computed theoretically the classical problem of forced convection flow adjacent to a slender needle. In addition, this work is subject to the variable surface temperature. A few years later, Hayat *et al.,* [26] studied the stagnation point flow of water-carbon nanoliquid by considering the variable heat flux on the needle surface. In recent times, many works have been performed to study the thin needle in nanofluid. For instance, Krishna *et al.,* [27], Ahmad *et al.,* [28] and Salleh *et al.,* [29] using different physical effects. In addition, Salleh *et al.,* [30] analyzed the impacts of buoyancy force and combined nanomaterials on nanoliquid flow towards a thin needle by performing stability analysis. The concept of stability analysis has been triggered by Merkin [31] in 1985. He presumed that it is necessary to compute the stability of the solution if there exists more than one solution. Since the pioneering work of Merkin [31], most of the researchers have taken an opportunity to consider stability analysis in their studies [32-36].

Motivated by the previous researches, the intention here is to examine the behavior of hybrid nanofluid due to horizontal slender needle. In this study, the needle is considered to move in the

same or reverse way of free stream flow. By using suitable transformations, similarity equations are formulated and computed numerically via bvp4c function with the help of MATLAB software. Graphical illustrations are shown to explain the role of the embedded parameters in the flow system.

2. Model Description

We examine a steady laminar flow and heat transfer adjacent to a moving slender needle immersed in hybrid nanoliquid at a constant ambient temperature T_∞. The needle surface is kept at uniform temperature T_n such that $T_n > T_\infty$. The cylindrical coordinate system for the axial and radial of the needle are represented by x and r, respectively, in which $r = R(x)$ refers to the radius of the needle. In the case of moving slender needle, we assumed the needle moves with a uniform velocity U_n in the opposite or same way of the free stream that have a uniform velocity U_∞. Following the standard boundary layer presumptions, the appropriate governing equations of the current flow are [27]

$$(ru)_x + (rv)_r = 0, \tag{1}$$

$$u_t + uu_x + vu_r = \frac{\mu_{hnf}}{\rho_{hnf}}\frac{1}{r}(ru_r)_r, \tag{2}$$

$$T_t + uT_x + vT_r = \frac{\alpha_{hnf}}{r}(rT_r)_r, \tag{3}$$

associate with the following boundary conditions

$$t < 0: u(x,r,t) = v(x,r,t) = 0, T(x,r,t) = T_\infty,$$

$$t \geq 0: u(x,r,t) = U_n,\ v(x,r,t)=0,\ T(x,r,t) = T_n \text{ at } r = R(x),$$

$$u(x,r,t) \to U_\infty, T(x,r,t) \to T_\infty \text{ as } r \to \infty, \tag{4}$$

with u and v being the velocities for x and r axis, respectively, t is the time for unsteady-state flow and T is the fluid temperature. Here μ, ρ, k, α and ρC_p represent the dynamic viscosity, density, thermal conductivity, thermal diffusivity and volumetric heat capacity where the subscripts hnf, f, n, s_1 and s_2 refer to the hybrid nanofluid, base fluid, condition at the needle surface, solid nanoparticles of alumina and copper, respectively. In addition, the heat capacity at the uniform pressure of the base fluid is denoted as C_p, and alumina and copper nanoparticle volume fractions are respectively, ϕ_1 and ϕ_2. When $\phi_1 = \phi_2 = 0$, it is corresponds to a regular fluid. The applied relations for physical properties of hybrid nanoliquid and nanoliquid are presented in Table 1 (Devi and Devi [9]). Meanwhile, the thermophysical characteristics of the nanoparticles and water at $25^\circ C$ are tabulated in Table 2 (Oztop and Abu-Nada [37])

Table 1
Applied relations for physical properties of hybrid nanoliquid and nanoliquid

Properties	Nanofluid	Hybrid Nanofluid
Heat capacity	$(\rho C_p)_{nf} = (1-\phi)(\rho C_p)_f + \phi(\rho C_p)_s$	$(\rho C_p)_{hnf} = (1-\phi_2)\left[(1-\phi_1)(\rho C_p)_f + \phi_1(\rho C_p)_{s_1}\right] + \phi_2(\rho C_p)_{s_2}$
Thermal Conduc-tivity	$\frac{k_{nf}}{k_f} = \frac{k_s + 2k_f - 2\phi(k_f - k_s)}{k_s + 2k_f + \phi(k_f - k_s)}$	$\frac{k_{hnf}}{k_{bf}} = \frac{k_{s_2} + 2k_{bf} - 2\phi_2(k_{bf} - k_{s_2})}{k_{s_2} + 2k_{bf} + \phi_2(k_{bf} - k_{s_2})}$, where $\frac{k_{bf}}{k_f} = \frac{k_{s_1} + 2k_f - 2\phi_1(k_f - k_{s_1})}{k_{s_1} + 2k_f + \phi_1(k_f - k_{s_1})}$
Dynamic viscosity	$\mu_{nf} = \frac{\mu_f}{(1-\phi)^{2.5}}$	$\mu_{hnf} = \frac{\mu_f}{(1-\phi_1)^{2.5}(1-\phi_2)^{2.5}}$
Density	$\rho_{nf} = (1-\phi)\rho_f + \phi\rho_s$	$\rho_{hnf} = (1-\phi_2)\left[(1-\phi_1)\rho_f + \phi_1\rho_{s_1}\right] + \phi_2\rho_{s_2}$

Table 2
Thermophysical properties of nanoparticles and water at 25°C

Properties	Water	Al_2O_3	Cu
$\rho\ (kg/m^3)$	997.0	3970	8933
C_p(J/kg K)	4180	765	385
$k\ (W/mK)$	0.6071	40	400

In computing the numerical solution for this problem, we first consider the steady-state flow where $t = 0$, hence, $\partial u/\partial t$ and $\partial T/\partial t$ both are equal to zero. Now, we seek for the following similarity transformations

$$\psi(x,r) = \nu_f x f(\eta), \theta(\eta) = \frac{T-T_\infty}{T_n-T_\infty}, \eta = \frac{Ur^2}{\nu_f x}, \tag{5}$$

in which η, $\theta(\eta)$, $\psi(x,r)$, ν_f and $U = U_n + U_\infty$ are the similarity variable, dimensionless temperature, dimensionless stream function, fluid kinematic viscosity and composite velocity of the needle and free stream flow, respectively. By using the given stream function, the velocity components of u and v are given by

$$u = \frac{1}{r}\frac{\partial \psi}{\partial r}, v = -\frac{1}{r}\frac{\partial \psi}{\partial x}, \tag{6}$$

that fulfill Eq. (1) identically. The thickness and the shape of the needle can be stipulated through the above equation by assuming $\eta = c$ which denotes the needle size or thickness, where its surface is defined as

$$R(x) = \left(\frac{\nu_f c x}{U}\right)^{1/2}. \tag{7}$$

Using Eq. (5) and (6) into Eq. (2) to (4) yield the differential equations below

$$\frac{1}{B_1 B_2}(2\eta f''' + 2f'') + ff'' = 0, \tag{8}$$

$$\frac{2C_1}{\Pr C_2}(\eta\theta'' + \theta') + f\theta' = 0, \tag{9}$$

where

$$B_1 = (1-\phi_1)^{2.5}(1-\phi_2)^{2.5}, B_2 = (1-\phi_2)\left[(1-\phi_1)+\phi_1\frac{\rho_{s1}}{\rho_f}\right]+\phi_2\frac{\rho_{s2}}{\rho_f},$$

$$C_1 = \frac{k_{hnf}}{k_f} = \frac{k_{s2}+2C_0k_f-2\phi_2(C_0k_f-k_{s2})}{k_{s2}+2C_0k_f+\phi_2(C_0k_f-k_{s2})}C_0 \text{ where } C_0 = \frac{k_{s1}+2k_f-2\phi_1(k_f-k_{s1})}{k_{s1}+2k_f+\phi_1(k_f-k_{s1})},$$

$$C_2 = (1-\phi_2)\left[(1-\phi_1)+\phi_1\frac{(\rho C_p)_{s1}}{(\rho C_p)_f}\right]+\phi_2\frac{(\rho C_p)_{s2}}{(\rho C_p)_f},$$

in which prime is the differentiation with respect to η. The boundary conditions for the above equations are

$$f(c) = \frac{\varepsilon}{2}c, f'(c) = \frac{\varepsilon}{2}, \theta(c) = 1,$$

$$f'(\eta) \to \frac{1}{2}(1-\varepsilon), \theta(\eta) \to 0 \text{ as } \eta \to \infty. \quad (10)$$

Here $\varepsilon = U_n/U$ is a velocity ratio parameter within the needle and fluid flow and $\Pr = \nu_f/\alpha_f$ is the Prandtl number. The physical quantities such as the coefficient of skin friction C_f and local Nusselt number Nu_x are formulated as

$$C_f = \frac{\tau_n}{\rho_f U^2}, Nu_x = \frac{xq_n}{k_f(T_n-T_\infty)}, \quad (11)$$

and the shear stress τ_n and the heat flux q_n are as follows

$$\tau_n = \mu_{hnf}(u_r)_{r=c}, q_n = -k_{hnf}(T_r)_{r=c}. \quad (12)$$

Introducing Eq. (5) and (12) into Eq. (11) yields

$$(\mathrm{Re}_x)^{1/2}C_f = \frac{4c^{1/2}}{(1-\phi_1)^{2.5}(1-\phi_2)^{2.5}}f''(c), (\mathrm{Re}_x)^{-1/2}Nu_x = -\frac{2k_{hnf}}{k_f}c^{1/2}\theta'(c), \quad (13)$$

where $\mathrm{Re}_x = Ux/\nu_f$ is the local Reynolds number.

3. Analysis of Stability

After obtaining the numerical solutions, we found that there exists a multiple solution called dual solutions. In identifying which of the solutions are numerically stable, we conducted a stability analysis. The problems considering the stability analysis has been done by several authors such as Weidman *et al.,* [32] and also Rosca and Pop [34]. It is observed from their works that the stable flow represented by upper branch solutions, meanwhile the results are invertible for the lower branch solution. In contrast to the finding of numerical solutions, in this section we consider unsteady-state

flow as in Eq. (2) to (4) by initiating the dimensionless time variable $\tau = 2Ut/x$. Hence, the similarity transformations (5) can be rewritten as

$$\psi(x,r) = \nu_f x f(\eta,\tau), \theta(\eta,\tau) = \frac{T-T_\infty}{T_n-T_\infty}, \eta = \frac{Ur^2}{\nu_f x}, \tau = \frac{2Ut}{x}. \tag{14}$$

From the above equation, the purpose of τ is related to the initial value problem that is consistent with the solution that will be attained in practice or the solution is said to be physically realizable. Next, replacing Eq. (14) into Eq. (2) to (4) yield the following

$$\frac{2}{B_1 B_2}\left[\eta\frac{\partial^3 f}{\partial\eta^3} + \frac{\partial^2 f}{\partial\eta^2}\right] - \frac{\partial^2 f}{\partial\eta\partial\tau} + \tau\frac{\partial^2 f}{\partial\eta\partial\tau}\frac{\partial f}{\partial\eta} - \tau\frac{\partial^2 f}{\partial\eta^2}\frac{\partial f}{\partial\tau} + f\frac{\partial^2 f}{\partial\eta^2} = 0, \tag{15}$$

$$\frac{2C_1}{\mathrm{Pr}C_2}\left[\eta\frac{\partial^2\theta}{\partial\eta^2} + \frac{\partial\theta}{\partial\eta}\right] + \tau\frac{\partial f}{\partial\eta}\frac{\partial\theta}{\partial\tau} - \tau\frac{\partial f}{\partial\tau}\frac{\partial\theta}{\partial\eta} + f\frac{\partial\theta}{\partial\eta} - \frac{\partial\theta}{\partial\tau} = 0, \tag{16}$$

and the boundary conditions become

$$f(c,\tau) = \frac{\varepsilon}{2}c + \tau\frac{\partial f}{\partial\tau}(c,\tau), \frac{\partial f}{\partial\eta}(c,\tau) = \frac{\varepsilon}{2}, \theta(c,\tau) = 1,$$

$$\frac{\partial f}{\partial\eta}(\eta,\tau) \to \frac{1-\varepsilon}{2}, \theta(\eta,\tau) \to 0 \text{ as } \eta \to \infty. \tag{17}$$

Afterward, introducing [32]

$$f(\eta,\tau) = f_0(\eta) + e^{-\gamma\tau}F(\eta,\tau), \theta(\eta,\tau) = \theta_0(\eta) + e^{-\gamma\tau}G(\eta,\tau), \tag{18}$$

to determine the stability of the output $f = f_0(\eta)$ and $\theta = \theta_0(\eta)$ that meet the boundary value problem in Eq. (15) to (17). In the above equation, γ represents the eigenvalue parameter and the small relative to $f_0(\eta)$ and $\theta_0(\eta)$ are respectively given by $F(\eta,\tau)$ and $G(\eta,\tau)$. Now, replacing Eq. (18) into Eq. (15) to (17) to obtain the linear eigenvalue equations as follows

$$\frac{2}{B_1 B_2}(\eta F_0''' + F_0'') + f_0 F_0'' + F_0 f_0'' + \gamma F_0' = 0, \tag{19}$$

$$\frac{2C_1}{\mathrm{Pr}C_2}(\eta G_0'' + G_0') + f_0 G_0' + F_0\theta_0' + \gamma G_0 = 0, \tag{20}$$

subject to the conditions

$$F_0(c) = 0, F_0'(c) = 0, G_0(c) = 0,$$

$$F_0'(\eta) \to 0, G_0(\eta) \to 0 \text{ as } \eta \to \infty. \tag{21}$$

To proceed with the next step, we have to assume $\tau = 0$ corresponds to an initial growth or decay of the output (18). Hence, the functions $F(\eta,\tau)$ and $G(\eta,\tau)$ can be rewritten as $F_0(\eta)$ and $G_0(\eta)$, respectively. The solutions of Eq. (19) and (20) will give an infinite set of eigenvalues γ. Thus, Harris *et al.,* [33] suggest that the region of the eigenvalue can be computed by choosing to relax the

condition on $F_0{}'(\eta)$ or $G_0(\eta)$. In the current analysis, we decide to relax the condition on $F_0{}'(\eta) \to 0$ as $\eta \to \infty$, and solve numerically the Eq. (19) to (21) together with the new condition $F_0{}''(c) = 1$.

4. Interpretation of Results

The focus of this section is to explore the influences of parameters like nanoparticle volume fractions, needle thickness and velocity ratio or moving parameter on dimensionless local heat flux, shear stress, local Nusselt number, coefficient of skin friction, temperature as well as velocity profiles. The numerical outcomes of this study are solved and plotted in this section using bvp4c function in MATLAB. Bvp4c function is the implemented package use to compute the boundary value problem for ordinary differential equations. When applying the package, the solutions are gained through the initial guess which is given at the initial starting mesh point. We also have to change the step size in order to obtain the exact certainty.

Figure 1 and 2 are plotted to describe the effects of the pure water ($\phi_1 = \phi_2 = 0$), nanoliquid ($\phi_1 = 0.01, \phi_2 = 0$) and hybrid nanoliquid ($\phi_1 = \phi_2 = 0.02$) on the variation trends of local heat flux $-\theta'(c)$ and surface shear stress $f''(c)$. In certain region of $\varepsilon_c < \varepsilon \leq -0.6$, hybrid nanofluid gives the highest values of local heat flux as compared to a nanoliquid and pure water. This behavior occurs due to the reduction of thermal boundary layer thickness at the needle surface (see Figure 3). The fact that the combination of two types of nanoparticles gives better thermophysical properties, especially thermal conductivity, and this is why hybrid nanofluid shows excellent performance on local heat flux compared to others. However, it should be noted that outside this region ($\varepsilon_c < \varepsilon \leq -0.6$), the invertible result is found. The reason behind this is that when the needle is about to move in a similar direction as the free stream flow ($\varepsilon > 0$), the ratio of velocity has suddenly increased. This consequently causes the fluid to flow quickly and the composite nanoparticles difficult to form a stable suspension. Hence, it diminishes the local heat flux for hybrid nanofluid. Similarly, it is noted from Figure 2 that in a certain domain of $-2.1 \leq \varepsilon \leq 0.5$, hybrid nanofluid obtains a higher magnitude of shear stress than nanofluid and water. This happens due to the reduction of velocity boundary layer thickness at the needle wall (see Figure 4). When the needle moves in the opposite way of free stream flow ($\varepsilon < 0$), the ratio of velocity between the needle and the flow seems to be decreased. As a consequence, slow down the movement of the needle and causes more shear stress to occur on the wall. It is worth noticing that dual solutions appear when the needle moves with a smaller rate of velocity ratio parameter ($\varepsilon < 0$).

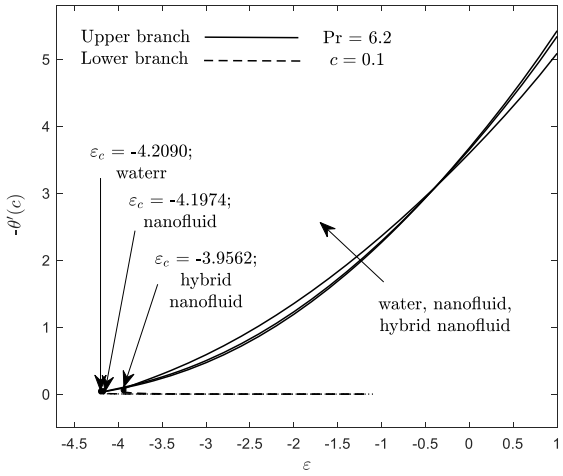

Fig. 1. Variation of ϕ_1 and ϕ_2 on local heat flux

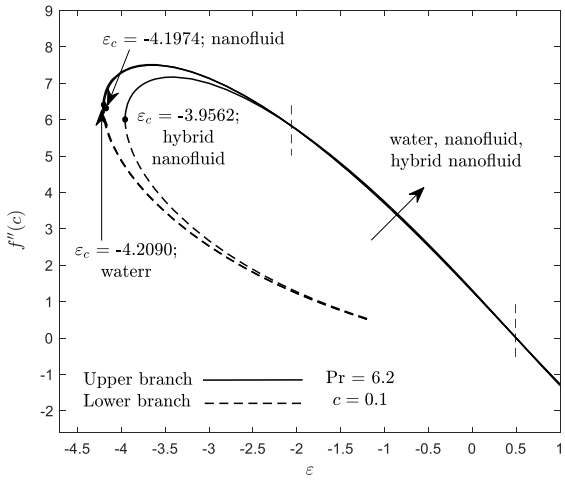

Fig. 2. Variation of ϕ_1 and ϕ_2 on shear stress

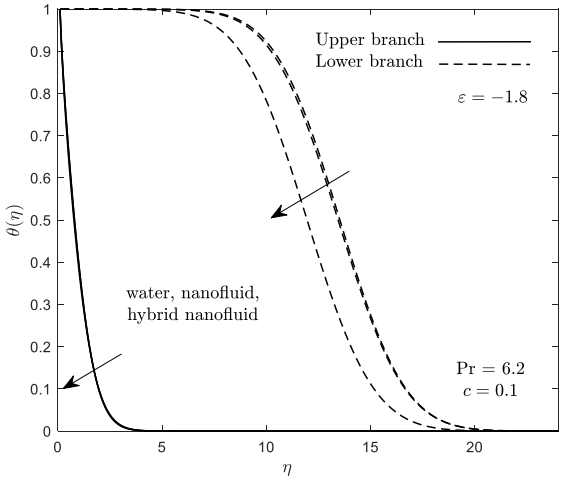

Fig. 3. Variation of ϕ_1 and ϕ_2 on temperature profiles

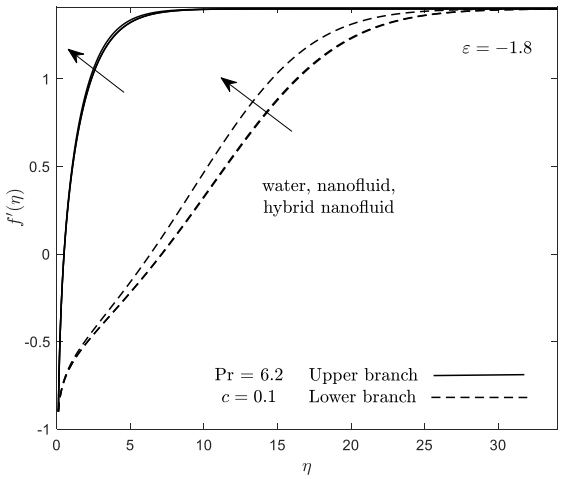

Fig. 4. Variation of ϕ_1 and ϕ_2 on velocity profiles

The influence of the copper nanoparticle rate ϕ_2 on the local heat fluxes $-\theta'(c)$ and surface shear stresses $f''(c)$ with velocity ratio parameter is presented in Figure 5 and 6 when $\phi_1 = 0.01$. From these figures, it is seen that an increment in the parameter ϕ_2 leads to increase the local heat flux and shear stress in certain regions of $\varepsilon_c < \varepsilon \leq -0.3$ and $-2.1 \leq \varepsilon \leq 0.4$, respectively. The explanation of the behavior of $-\theta'(c)$ is similar to Figure 1. However, Figure 6 demonstrated that the presence of a higher rate of copper nanoparticles causes more drag force to exist on the wall, and consequently, increases the shear stress. This is due to the collision of those nanoparticles in the system. Figure 7 and 8 depict the temperature and velocity distributions of the flow when the copper nanoparticle rate is changing. Noticeably, the profiles for the temperature and velocity obtained in this study has fulfilled the endpoint boundary condition asymptotically. Hence, the code used in the present study has been confirmed.

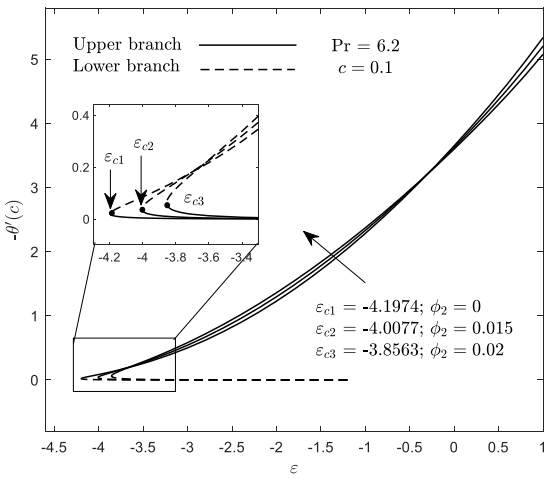

Fig. 5. Variation of ϕ_2 on local heat flux

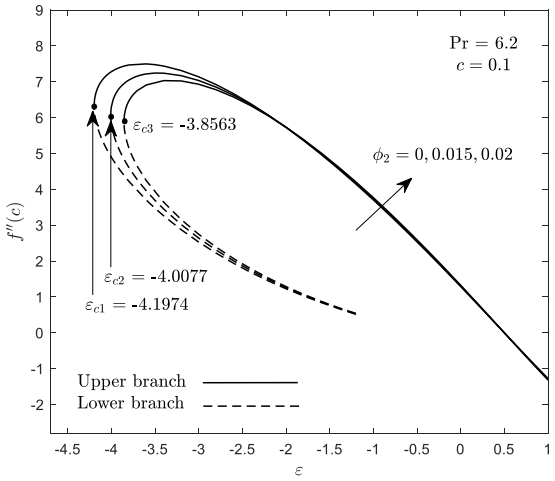

Fig. 6. Variation of ϕ_2 on shear stress

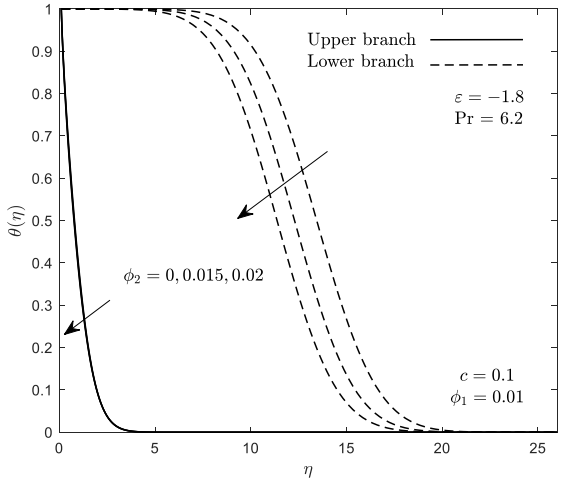

Fig. 7. Variation of ϕ_2 on temperature profiles

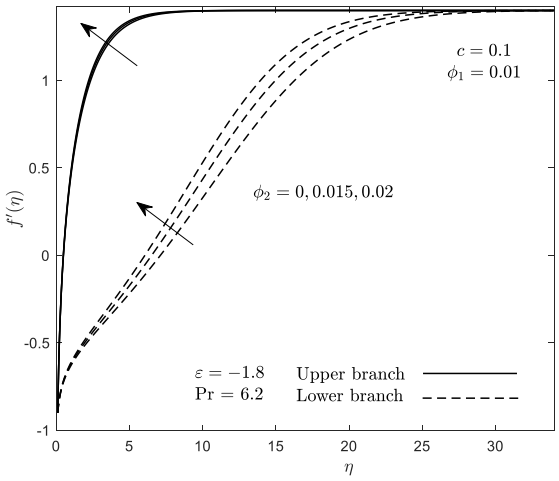

Fig. 8. Variation of ϕ_2 on velocity profiles

The computational values of heat transfer rate or local Nusselt number $(Re_x)^{-1/2}Nu_x$ and skin friction coefficient $(Re_x)^{1/2}C_f$ are shown in Figure 9 and 10 with various values of needle thicknesses c when $\phi_1 = \phi_2$. Besides that, Figure 11 and 12 illustrate the temperature and velocity fields for various needle thickness. As expected from Figure 9 and 10, the thin surface of the needle $(c = 0.05)$ gives larger magnitudes of local Nusselt number and skin friction coefficient. The reason for this is that the thinner wall faster the heat transfers between the fluid flow and the surface. This situation can be proved by the decrement of the thermal boundary layer thickness as the values of c decrease as shown in Figure 11. The thinner the thermal boundary layer thickness, the faster the rate of heat transfer. Besides, the momentum boundary layer thickness in Figure 12 seem to decrease as the parameter c decrease. This characteristic tends to enhance the surface shear stress, and as a result, accelerates the skin friction coefficient. Additionally, it is observed from Figure 9 and 10 that the magnitudes of the heat transfer and skin friction coefficient increase quadratically when the size of nanoparticles (ϕ_1 and ϕ_2) getting bigger. Physically, the addition of two kinds of nanoparticles in the base fluid causes more friction to occur on the surface. It is important to note that the existence of nanoparticles provides a greater surface area to volume ratio due to a large number of molecules on the boundaries. This behavior makes them highly stable in suspension, and consequently, augments the thermal conductivity and also the heat transfer rate.

The result of the stability analysis is represented by minimum eigenvalues γ as can be seen in Table 3. In this table, we computed several values of the nanoparticle volume fraction of alumina and copper, ϕ_1 and ϕ_2 respectively, when the velocity ratio parameter ε is changing in order to see the feature of the disturbance occur in the system. It is worth noticing that the positive sign of γ indicates an initial decay of disturbance which represent the stable solution. In contrast to that, the solution is unstable and there is an initial growth of the disturbance when γ takes the negative sign. The stable flow or solution always can be realizable in term of physical meaning.

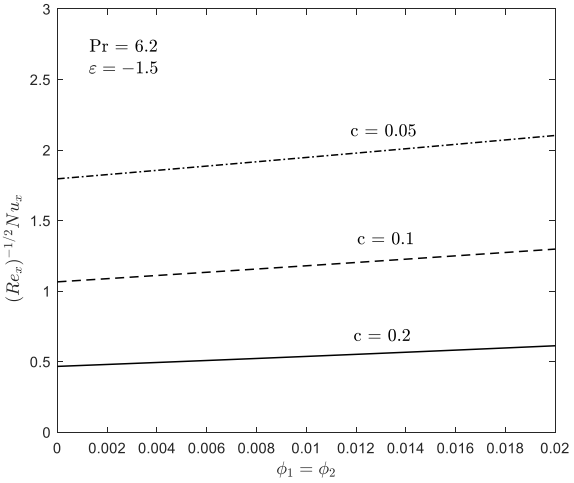

Fig. 9. Variation of c on local Nusselt number when $\phi_1 = \phi_2$

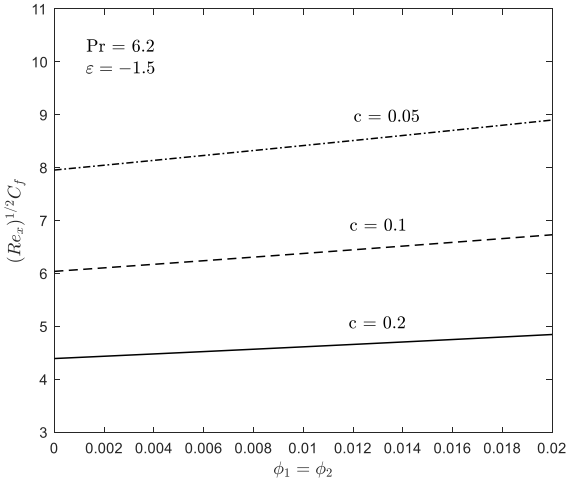

Fig. 10. Variation of c on skin friction coefficient when $\phi_1 = \phi_2$

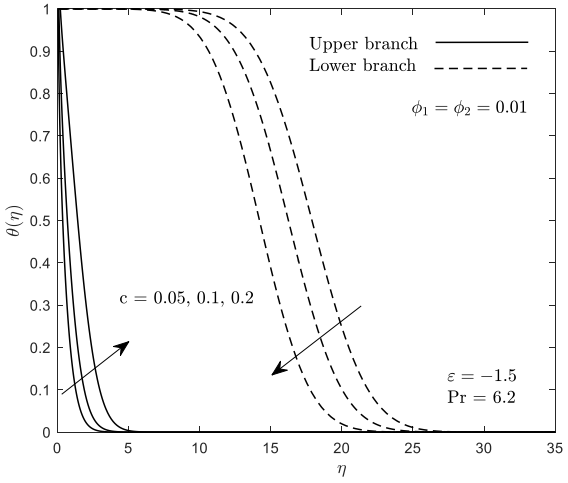

Fig. 11. Variation of c on temperature profiles

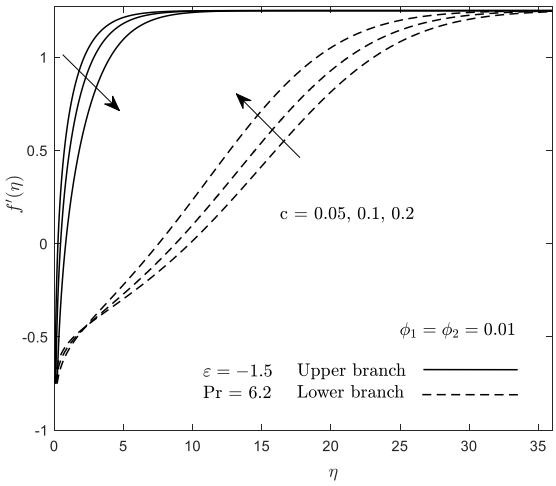

Fig. 12. Variation of c on velocity profiles

Table 3
Minimum eigenvalues γ for some values of ϕ_1, ϕ_2 and ε when $c = 0.1$ and $\Pr = 6.2$

ϕ_1 and ϕ_2	ε	Upper branch solution	Lower branch solution
$\phi_1 = \phi_2 = 0$	-4.18	0.0830	-0.0764
	-4.186	0.0737	-0.0684
	-4.1864	0.0730	-0.0679
$\phi_1 = 0.01, \phi_2 = 0$	-4.17	0.0805	-0.0743
	-4.173	0.0758	-0.0703
	-4.1736	0.0749	-0.0695
$\phi_1 = \phi_2 = 0.01$	-3.92	0.0921	-0.0836
	-3.925	0.0853	-0.0780
	-3.9258	0.0841	-0.0770

5. Final Remarks

This work studies the characteristics of the flow and heat transfer passing through a very thin needle immersed in a hybrid nanoliquid. The numerical results of this work are primarily relying upon the nanoparticle volume fractions of copper and alumina, the thickness of the needle and velocity ratio parameters. The key outcomes of this present work can be established in the following lines

i. The fluid with the composite nanoparticles possess higher magnitudes of local Nusselt number and skin friction compared to nanofluid and pure water.
ii. The higher rate of copper nanoparticles volume fraction ϕ_2 enhances the local heat flux and shear stress on the wall when ϕ_1 is kept at constant.
iii. The numerical values of heat transfer and skin friction coefficient increase as the surface of the needle become thinner.
iv. The flow where the needle opposes the free stream direction $\varepsilon < 0$ contributes to the existence of multiple solutions.
v. The lower branch solution indicated an unstable solution, whereas the upper branch solution indicated a stable solution.

Acknowledgement
Support of this research by the Universiti Putra Malaysia under Putra Grant GP IPS/2018/9667900 and Ministry of Higher Education Malaysia under Fundamental Research Grant Scheme FRGS/1/2018/STG06/UPM/02/4/ 5540155 is gratefully acknowledged.

References

[1] Jena, P. K., E. A. Brocchi, and M. S. Motta. "In-situ formation of Cu–Al2O3 nano-scale composites by chemical routes and studies on their microstructures." *Materials Science and Engineering: A* 313, no. 1-2 (2001): 180-186. https://doi.org/10.1016/S0921-5093(00)01998-5
[2] Suresh, S., Venkitaraj, K.P., Selvakumar, P., and Chandrasekar, M. "Synthesis of Al_2O_3-Cu/water hybrid nanofluids using two step method and its thermo physical properties." *Colloids and Surfaces A: Physicochemical and Engineering Aspects* 388, no. 1-3 (2011): 41-48. https://doi.org/10.1016/j.colsurfa.2011.08.005
[3] Nine, M.J., Munkhbayar, B., Rahman, M.S., Chung, H., and Jeong, H. "Highly productive synthesis process of well dispersed Cu_2O and Cu/Cu_2O nanoparticles and its thermal characterization." *Materials Chemistry and Physics* 141, no. 2-3 (2013): 636-642. https://doi.org/10.1016/j.matchemphys.2013.05.032
[4] Madhesh, D., Parameshwaran, R., and Kalaiselvam, S. "Experimental investigation on convective heat transfer and rheological characteristics of Cu-TiO_2 hybrid nanofluids." *Experimental Thermal and Fluid Science* 52 (2014): 104-115. https://doi.org/10.1016/j.expthermflusci.2013.08.026
[5] Afrand, M., Toghraie, D., and Sina, N. "Experimental study on thermal conductivity of water-based Fe3O4 nanofluid: development of a new correlation and modeled by artificial neural network." *International Communications in Heat and Mass Transfer* 75 (2016): 262-269. https://doi.org/10.1016/j.icheatmasstransfer.2016.04.023
[6] Esfe, M.H., Alirezaie, A., and Rejvani, M. "An applicable study on the thermal conductivity of SWCNT-MgO hybrid nanofluid and price-performance analysis for energy management." *Applied Thermal Engineering* 111 (2017): 1202-1210. https://doi.org/10.1016/j.applthermaleng.2016.09.091
[7] Takabi, T., and Salehi, S. "Augmentation of the heat transfer performance of a sinusoidal corrugated enclosure by employing hybrid nanofluid." *Advances in Mechanical Engineering* 6 (2014): 1-16. https://doi.org/10.1155/2014/147059
[8] Moghadassi, A., Ghomi, E., and Parvizian, F. "A numerical study of water based Al_2O_3 and Al_2O_3-Cu hybrid nanofluid effect on forced convective heat transfer." *International Journal of Thermal Sciences* 92 (2015): 50-57. https://doi.org/10.1016/j.ijthermalsci.2015.01.025

[9] Devi, S.S.U, and Devi, S.P.A. "Numerical investigation of three-dimensional hybrid Cu-Al_2O_3/water nanofluid flow over a stretching sheet with effecting Lorentz force subject to Newtonian heating." *Canadian Journal of Physics* 94, no. 5 (2016): 490-496. https://doi.org/10.1139/cjp-2015-0799

[10] Mehryan, S.A.M., Kashkooli, F.M., Ghalambaz, M., and Chamkha, A.J. "Free convection of hybrid Al_2O_3-Cu water nanofluid in a differentially heated porous cavity." *Advanced Powder Technology* 28, no. 9 (2017): 2295-2305. https://doi.org/10.1016/j.apt.2017.06.011

[11] Rashad, A.M., Rashidi, M.M., Lorenzini, G., Ahmed, S.E., and Aly, A.M. "Magnetic field and internal heat generation effects on the free convection in a rectangular cavity filled with a porous medium saturated with Cu-water nanofluid." *International Journal of Heat and Mass Transfer* 104 (2017): 878-889. https://doi.org/10.1016/j.ijheatmasstransfer.2016.08.025

[12] Hussain, S., Ahmed, S.E., and Akbar, T. "Entropy generation analysis in MHD mixed convection of hybrid nanofluid in an open cavity with a horizontal channel containing an adiabatic obstacle." *International Journal of Heat and Mass Transfer* 114 (2017): 1054-1066. https://doi.org/10.1016/j.ijheatmasstransfer.2017.06.135

[13] Hayat, T., and Nadeem, S. "Heat transfer enhancement with Ag-CuO/water hybrid nanofluid." *Results in Physics* 7 (2017): 2317-2324. https://doi.org/10.1016/j.rinp.2017.06.034

[14] Yousefi, M., Dinarvand, S., Yazdi, M.E., and Pop, I. "Stagnation point flow of an aqueous titania-copper hybrid nanofluid toward a wavy cylinder." *International Journal of Numerical Methods for Heat & Fluid Flow* 28, no. 7 (2018): 1716-1735. https://doi.org/10.1108/HFF-01-2018-0009

[15] Iqbal, Z., Akbar, N.S., Azhar, E., and Maraj, E.N. "Performance of hybrid nanofluid (Cu-CuO/water) on MHD rotating transport in oscillating vertical channel inspired by Hall current and thermal radiation." *Alexandria Engineering Journal* 57 (2018): 1943-1954. https://doi.org/10.1016/j.aej.2017.03.047

[16] Mansour, M.A., Siddiqa, S., Gorla, R.S.R., and Rashad, A.M. "Effects of heat source and sink on entropy generation and MHD natural convection of Al2O3-Cu/water hybrid nanofluid filled with square porous cavity." *Thermal Science and Engineering Progress* 6 (2018): 57-71. https://doi.org/10.1016/j.tsep.2017.10.014

[17] Lee, L.L. "Boundary layer over a thin needle." *The physics of fluids* 10, no. 4 (1967): 820-822. https://doi.org/10.1063/1.1762194

[18] Narain, J.P, and Mahinder S.U. "Forced heat transfer over thin needles." *Journal of Heat Transfer* 94, no. 2 (1972): 240-242. https://doi.org/10.1115/1.3449910

[19] Narain, J.P., and Mahinder S.U. "Combined forced and free-convection over thin needles." *International Journal of Heat and Mass Transfer* 16, no. 8 (1973): 1505-1512. https://doi.org/10.1016/0017-9310(73)90179-8

[20] Chen, J. L. S., and T. N. Smith. "Forced convection heat transfer from nonisothermal thin needles." *Journal of Heat Transfer* 100, no. 2 (1978): 358-362. https://doi.org/10.1115/1.3450809

[21] Kumari, M., and Nath, G. "Mixed convection boundary layer flow over a thin vertical cylinder with localized injection/suction and cooling/heating." *International Journal of Heat and Mass Transfer* 47 (2004): 969-976. https://doi.org/10.1016/j.ijheatmasstransfer.2003.08.014

[22] Ishak, Anuar, Roslinda Nazar, and Ioan Pop. "Boundary layer flow over a continuously moving thin needle in a parallel free stream." *Chinese Physics Letters* 24, no. 10 (2007): 2895. https://doi.org/10.1088/0256-307X/24/10/051

[23] Bano, N., and Singh, B.B. "An integral treatment for coupled heat and mass transfer by natural convection from a radiating vertical thin needle in a porous medium." *International Communications in Heat and Mass* Transfer 84 (2017): 41-48. https://doi.org/10.1016/j.icheatmasstransfer.2017.03.007

[24] Afridi, M.I., and Qasim, M. "Entropy generation and heat transfer in boundary layer flow over a thin needle moving in a parallel stream in the presence of nonlinear Rosseland radiation." *International Journal of Thermal Sciences* 123 (2018): 117-128. https://doi.org/10.1016/j.ijthermalsci.2017.09.014

[25] Grosan, T., and I. Pop. "Forced convection boundary layer flow past nonisothermal thin needles in nanofluids." *Journal of Heat Transfer* 133, no. 5 (2011): 054503.

https://doi.org/10.1115/1.4003059

[26] Hayat, T., Khan, M.I., Farooq, M., Yasmeen, T., and Alsaedi, A. "Water-carbon nanofluid flow with variable heat flux by a thin needle." *Journal of Molecular Liquids* 224 (2016): 786-791. https://doi.org/10.1016/j.molliq.2016.10.069

[27] Krishna, P.M., Sharma, R.P., and Sandeep, N. "Boundary layer analysis of persistent moving horizontal needle in Blasius and Sakiadis magnetohydrodynamic radiative nanofluid flows." *Nuclear Engineering and Technology* 49 (2017): 1654-1659. https://doi.org/10.1016/j.net.2017.07.023

[28] Ahmad, R., Mustafa, M., and Hina, S. "Buongiorno's model for fluid flow around a moving thin needle in a flowing nanofluid: A numerical study." *Chinese journal of physics* 55, no. 4 (2017): 1264-1274. https://doi.org/10.1016/j.cjph.2017.07.004

[29] Salleh, Siti Nur Alwani, Norfifah Bachok, Norihan Md Arifin, and Fadzilah Md Ali. "Slip Effect on Mixed Convection Flow Past a Thin Needle in Nanofluid Using Buongiorno's Model." *Journal of Advanced Research in Fluid Mechanics and Thermal Sciences* 59, no. 2 (2019): 243-253.

[30] Salleh, S.N.A, Bachok, N., Arifin, N.M., and Ali, F.M. "Effect of buoyancy force on the flow and heat transfer around a thin needle in Al_2O_3-Cu hybrid nanofluid." *CFD Letters* 12, no. 1 (2020): 22-36.

[31] Merkin, J.H. "On dual solutions occurring in mixed convection in a porous medium." *Journal of engineering Mathematics* 20, no. 2 (1986): 171-179. https://doi.org/10.1007/BF00042775

[32] Weidman, P.D., Kubitschek, D.G. and Davis, A.M.J. "The effect of transpiration on self-similar boundary layer flow over moving surfaces." *International journal of engineering science* 44, no. 11-12 (2006): 730-737. https://doi.org/10.1016/j.ijengsci.2006.04.005

[33] Harris, S.D., Ingham, D.B. and Pop. I. "Mixed convection boundary-layer flow near the stagnation point on a vertical surface in a porous medium: Brinkman model with slip." *Transport in Porous Media* 77, no. 2 (2009): 267-285. https://doi.org/10.1007/s11242-008-9309-6

[34] Rosca, A.V., and Pop, I. "Flow and heat transfer over a vertical permeable stretching/shrinking sheet with a second order slip. " *International Journal of Heat and Mass Transfer* 60 (2013): 355-364. https://doi.org/10.1016/j.ijheatmasstransfer.2012.12.028

[35] Bakar, N.A.A, Bachok, N., Arifin N.M., and Pop, I. "Stability analysis on the flow and heat transfer of nanofluid past a stretching/shrinking cylinder with suction effect." *Results in Physics* 9 (2018): 1335-1344. https://doi.org/10.1016/j.rinp.2018.04.056

[36] Salleh, S.N.A, Bachok, N. and Arifin, N.M., "Stability analysis of a rotating flow toward a shrinking permeable surface in nanofluid." *Malaysian Journal of Science* 38, no. 1 (2019): 19-32. https://doi.org/10.22452/mjs.sp2019no1.2

[37] Oztop, H.F., and Abu-Nada, E. "Numerical study of natural convection in partially heated rectangular enclosures filled with nanofluids." *International journal of heat and fluid flow* 29, no. 5 (2008): 1326-1336. https://doi.org/10.1016/j.ijheatfluidflow.2008.04.009